Double and triple photoionization of Li and Be

J. Colgan,[1] M. S. Pindzola,[2] and F. Robicheaux[2]
[1]*Theoretical Division, Los Alamos National Laboratory, Los Alamos, New Mexico 87545, USA*
[2]*Department of Physics, Auburn University, Auburn, Alabama, 36849, USA*
(Received 20 April 2005; published 29 August 2005)

We present calculations for the double photoionization (with excitation) and the triple photoionization of Li and Be. We extend and more fully discuss the previous calculations made for Li by Colgan *et al.* [Phys. Rev. Lett. **93**, 053201 (2004)] and present calculations for Be. The Be triple photoionization cross sections are compared with previous double shake-off model calculations of Kheifets and Bray [J. Phys. B **36**, L211 (2003)], and our calculations are found to be significantly lower.

DOI: 10.1103/PhysRevA.72.022727 PACS number(s): 32.80.Fb, 34.50.Fa

I. INTRODUCTION

The last ten years or so have seen intensive efforts, both theoretically and experimentally, in the study of the three-body Coulomb problem found in the double photoionization of the helium atom. It is now the case that for total double photoionization cross sections and single, double, and triple differential cross sections, very good agreement is found between several different theoretical techniques and experimental measurements over a wide range of incident energies and electron energy and angle sharings. A review of early work on this topic has been given by Briggs and Schmidt [1] and the various recent important theoretical developments as well as some of the important experimental measurements are listed [2–7].

Subsequently, interest is growing in moving beyond the double photoionization of He. More complex targets, such as Be, have been examined by the convergent close-coupling method [8], the time-dependent close-coupling technique [9], and the hyperspherical *R*-matrix with semiclassical outgoing waves technique [10]. These have recently been supported by experimental measurements of the total double photoionization cross section for Be [11,12] in the near threshold region.

There is also increasing interest in examining the four-body Coulomb problem, most simply found in the triple photoionization of Li. This represents a much more difficult problem than the double photoionization of He, since now the motion of three electrons must be treated equally. Early experimental measurements were provided by Wehlitz *et al.* [13]. The triple photoionization cross section in the high-energy limit was studied by van der Hart and Greene [14], and a half-collision model was recently used [15] to examine the triple photoionization cross section and related ratios. Fairly good agreement was found between these model calculations and experiment. Recently, the time-dependent close-coupling method was used to treat all three electrons of Li equally, by propagating a nine-dimensional wave function according to the Schrödinger equation [16]. Double photoionization with excitation and triple photoionization cross sections were obtained which were in good agreement with experiment [13,17]. In this paper, we present further time-dependent calculations for Li and extend our method to examine the double and triple photoionization of Be. There has been a recent double shake-off model calculation for the triple photonionization of Be [18]. We compare our results with this calculation and also compare and contrast the double and triple photoionization cross sections of Li and Be.

In the next section we describe the time-dependent close-coupling theory as applied to triple photoionization calculations. We then present our results for double and triple photoionization of Li and Be. We conclude with a short summary of our work.

II. THEORY

The crucial equations for photoionization of a three-electron target atom were laid out in our previous paper on Li [16]. For the sake of completeness, we repeat these equations here and give the full form of all the relevant quantities. We note that this three-electron treatment has also been recently applied with success to the electron-impact single and double ionization of He [19] and also to the single and double autoionization of hollow atom states of Li [20].

For a three-electron target atom, the angular reduction of a weak-field form of the time-dependent Schrödinger equation yields a single set of time-dependent close-coupled partial differential equations

$$
\begin{aligned}
i\frac{\partial P^{\mathcal{L}}_{l_1 l_2 L l_3}(r_1,r_2,r_3,t)}{\partial t} &= T_{l_1 l_2 l_3}(r_1,r_2,r_3)P^{\mathcal{L}}_{l_1 l_2 L l_3}(r_1,r_2,r_3,t) \\
&+ \sum_{l_1',l_2',L',l_3'} \sum_{i<j}^{3} V^{\mathcal{L}}_{l_1 l_2 L l_3, l_1' l_2' L' l_3'}(r_i,r_j)P^{\mathcal{L}}_{l_1' l_2' L' l_3'}(r_1,r_2,r_3,t) \\
&+ \sum_{l_1',l_2',L',l_3'} \sum_{i}^{3} W^{\mathcal{L}\mathcal{L}_0}_{l_1 l_2 L l_3, l_1' l_2' L' l_3'}(r_i,t)\bar{P}^{\mathcal{L}_0}_{l_1' l_2' L' l_3'}(r_1,r_2,r_3), \qquad (1)
\end{aligned}
$$

where

$$
T_{l_1 l_2 l_3}(r_1,r_2,r_3) = \sum_{i}^{3}\left(-\frac{1}{2}\frac{\partial^2}{\partial r_i^2} + \frac{l_i(l_i+1)}{2r_i^2} - \frac{Z}{r_i}\right), \qquad (2)
$$

and the coupling operators are found by reduction of

$$V^{\mathcal{L}}_{l_1 l_2 L l_3, l_1' l_2' L' l_3'}(r_i, r_j) = \langle (((l_1, l_2)L, l_3)\mathcal{L} | (r_{ij})^{-1} | ((l_1', l_2')L', l_3')\mathcal{L}) \rangle \tag{3}$$

to expressions involving standard $3j$ and $6j$ symbols, given by

$$V^{\mathcal{L}}_{l_1 l_2 L l_3, l_1' l_2' L' l_3'}(r_1, r_2) = (-1)^{l_1 + l_1' + L} \delta_{l_3, l_3'} \delta_{L, L'} \sqrt{(2l_1+1)(2l_1'+1)(2l_2+1)(2l_2'+1)} \times \sum_{\lambda} \frac{(r_1, r_2)^{\lambda}_{<}}{(r_1, r_2)^{\lambda+1}_{>}} \begin{pmatrix} l_1 & \lambda & l_1' \\ 0 & 0 & 0 \end{pmatrix} \begin{pmatrix} l_2 & \lambda & l_2' \\ 0 & 0 & 0 \end{pmatrix} \begin{Bmatrix} l_1 & l_2 & \mathcal{L} \\ l_2' & l_1' & \lambda \end{Bmatrix}, \tag{4}$$

$$V^{\mathcal{L}}_{l_1 l_2 L l_3, l_1' l_2' L' l_3'}(r_1, r_3) = (-1)^{l_2 + \mathcal{L}} \delta_{l_2, l_2'} \sqrt{(2l_1+1)(2l_1'+1)(2l_3+1)(2l_3'+1)(2L+1)(2L'+1)} \times \sum_{\lambda} (-1)^{\lambda} \frac{(r_1, r_3)^{\lambda}_{<}}{(r_1, r_3)^{\lambda+1}_{>}} \begin{pmatrix} l_1 & \lambda & l_1' \\ 0 & 0 & 0 \end{pmatrix} \begin{pmatrix} l_3 & \lambda & l_3' \\ 0 & 0 & 0 \end{pmatrix} \begin{Bmatrix} L & l_3 & \mathcal{L} \\ l_3' & L' & \lambda \end{Bmatrix} \begin{Bmatrix} l_1 & l_2 & L \\ L' & \lambda & l_1' \end{Bmatrix}, \tag{5}$$

and

$$V^{\mathcal{L}}_{l_1 l_2 L l_3, l_1' l_2' L' l_3'}(r_2, r_3) = (-1)^{l_1' + l_2 + l_2' + L + L' + \mathcal{L}} \delta_{l_1, l_1'} \sqrt{(2l_2+1)(2l_2'+1)(2l_3+1)(2l_3'+1)(2L+1)(2L'+1)} \times \sum_{\lambda} (-1)^{\lambda} \frac{(r_2, r_3)^{\lambda}_{<}}{(r_2, r_3)^{\lambda+1}_{>}} \begin{pmatrix} l_2 & \lambda & l_2' \\ 0 & 0 & 0 \end{pmatrix} \begin{pmatrix} l_3 & \lambda & l_3' \\ 0 & 0 & 0 \end{pmatrix} \begin{Bmatrix} L & l_3 & \mathcal{L} \\ l_3' & L' & \lambda \end{Bmatrix} \begin{Bmatrix} l_1 & l_2 & L \\ \lambda & L' & l_2' \end{Bmatrix}. \tag{6}$$

The dipole radiation field coupling operators are also found by reduction of

$$W^{\mathcal{L}\mathcal{L}_0}_{l_1 l_2 L l_3, l_1' l_2' L' l_3'}(r_i, t) = g(r_i) F(t) \langle (((l_1, l_2)L, l_3)\mathcal{L} | \vec{C}^1(i) | ((l_1', l_2')L', l_3')\mathcal{L}_0 \rangle \tag{7}$$

to expressions involving standard $3j$ and $6j$ symbols given by

$$W^{\mathcal{L}\mathcal{L}_0}_{l_1 l_2 L l_3, l_1' l_2' L' l_3'}(r_1, t) = (-1)^{l_2 + l_3 + L + L' + \mathcal{L} + \mathcal{L}_0} \delta_{l_2, l_2'} \delta_{l_3, l_3'} \sqrt{(2l_1+1)(2l_1'+1)(2L+1)(2L'+1)(2\mathcal{L}+1)(2\mathcal{L}_0+1)} \times g(r_1) F(t) \begin{pmatrix} l_1 & 1 & l_1' \\ 0 & 0 & 0 \end{pmatrix} \begin{pmatrix} \mathcal{L} & 1 & \mathcal{L}_0 \\ 0 & 0 & 0 \end{pmatrix} \begin{Bmatrix} L & l_3 & \mathcal{L} \\ \mathcal{L}_0 & 1 & L' \end{Bmatrix} \begin{Bmatrix} l_1 & l_2 & L \\ L' & 1 & l_1' \end{Bmatrix}, \tag{8}$$

$$W^{\mathcal{L}\mathcal{L}_0}_{l_1 l_2 L l_3, l_1' l_2' L' l_3'}(r_2, t) = (-1)^{l_1 + l_2 + l_2' + l_3 + \mathcal{L} + \mathcal{L}_0} \delta_{l_1, l_1'} \delta_{l_3, l_3'} \sqrt{(2l_2+1)(2l_2'+1)(2L+1)(2L'+1)(2\mathcal{L}+1)(2\mathcal{L}_0+1)} \times g(r_2) F(t) \begin{pmatrix} l_2 & 1 & l_2' \\ 0 & 0 & 0 \end{pmatrix} \begin{pmatrix} \mathcal{L} & 1 & \mathcal{L}_0 \\ 0 & 0 & 0 \end{pmatrix} \begin{Bmatrix} L & l_3 & \mathcal{L} \\ \mathcal{L}_0 & 1 & L' \end{Bmatrix} \begin{Bmatrix} l_1 & l_2 & L \\ 1 & L' & l_2' \end{Bmatrix}, \tag{9}$$

and

$$W^{\mathcal{L}\mathcal{L}_0}_{l_1 l_2 L l_3, l_1' l_2' L' l_3'}(r_3, t) = (-1)^{l_3 + l_3' + L + 1} \delta_{l_1, l_1'} \delta_{l_2, l_2'} \delta_{L, L'} \sqrt{(2l_3+1)(2l_3'+1)(2\mathcal{L}+1)(2\mathcal{L}_0+1)} \times g(r_3) F(t) \begin{pmatrix} l_3 & 1 & l_3' \\ 0 & 0 & 0 \end{pmatrix} \begin{pmatrix} \mathcal{L} & 1 & \mathcal{L}_0 \\ 0 & 0 & 0 \end{pmatrix} \begin{Bmatrix} L & l_3 & \mathcal{L} \\ 1 & \mathcal{L}_0 & l_3' \end{Bmatrix}. \tag{10}$$

The time dependence of the linearly polarized electric field amplitude $F(t)$ is proportional to $\cos \omega t$, where ω is the radiation field frequency, while in the length gauge $g(r) = r$.

In Eq. (1) the function $\bar{P}^{\mathcal{L}_0}_{l_1' l_2' L' l_3'}(r_1, r_2, r_3)$ represents the radial part of the fully correlated initial $^2S^e$ ground state, and $P^{\mathcal{L}}_{l_1 l_2 L l_3}(r_1, r_2, r_3, t)$ represents the radial part of the fully correlated final state. The radial wave functions $\bar{P}^{\mathcal{L}_0}_{l_1' l_2' L' l_3'}(r_1, r_2, r_3)$ are obtained by relaxation of the Schrödinger equation in imaginary time for a three-electron target atom. Care must be taken to properly relax the wave function to the correct ground state. For Li, a fictitious $1s^3\ ^2S$ state was created and then a subsequent $1s^2 2s\ ^2S$ state was constructed, which was always kept orthogonal to the $1s^3$ state. The initial state used in this relaxation was a product state consisting of the Li^{2+} $(1s) \times (1s) \times (2s)$ states. For Be, a set of one-electron states were constructed in the field of a frozen-core Be^{3+} $(1s)$ state, found by diagonalization of

$$h(r) = -\frac{1}{2}\frac{\partial^2}{\partial r^2} + \frac{l(l+1)}{2r^2} + V(r), \tag{11}$$

where $V(r)$ is a Hartree-Slater potential that screens the Coulomb field. These Be^{2+} (nl) states were used as the initial

product state for the relaxation, i.e., Be^{2+} $(1s)\times(2s)\times(2s)$. To prevent this initial state from relaxing to any lower state containing two $1s$ electrons, a Schmidt orthogonalization procedure was employed at every imaginary time step:

$$\begin{aligned}\bar{P}^{\mathcal{L}_0}_{l_1'l_2'L'l_3'}(r_1,r_2,r_3,\tau) = \bar{P}^{\mathcal{L}_0}_{l_1'l_2'L'l_3'}(r_1,r_2,r_3,\tau) &- \int_0^\infty\int_0^\infty P_{1s}(r_1)P_{1s}(r_2)\bar{P}^{\mathcal{L}_0}_{l_1'l_2'L'l_3'}(r_1,r_2,r_3,\tau)dr_1dr_2 \times P_{1s}(r_1)P_{1s}(r_2)\delta_{l_1,0}\delta_{l_2,0}\\ &- \int_0^\infty\int_0^\infty P_{1s}(r_1)P_{1s}(r_3)\bar{P}^{\mathcal{L}_0}_{l_1'l_2'L'l_3'}(r_1,r_2,r_3,\tau)dr_1dr_3 \times P_{1s}(r_1)P_{1s}(r_3)\delta_{l_1,0}\delta_{l_3,0}\\ &- \int_0^\infty\int_0^\infty P_{1s}(r_2)P_{1s}(r_3)\bar{P}^{\mathcal{L}_0}_{l_1'l_2'L'l_3'}(r_1,r_2,r_3,\tau)dr_2dr_3 \times P_{1s}(r_2)P_{1s}(r_3)\delta_{l_2,0}\delta_{l_3,0}\\ &+ 2\int_0^\infty\int_0^\infty\int_0^\infty P_{1s}(r_1)P_{1s}(r_2)P_{1s}(r_3)\bar{P}^{\mathcal{L}_0}_{l_1'l_2'L'l_3'}(r_1,r_2,r_3,\tau)dr_1dr_2dr_3 \times P_{1s}(r_1)P_{1s}(r_2)P_{1s}(r_3)\delta_{l_1,0}\delta_{l_2,0}\delta_{l_3,0}.\end{aligned} \tag{12}$$

In this procedure, we orthogonalize the initial state $\bar{P}^{\mathcal{L}_0}_{l_1'l_2'L'l_3'}(r_1,r_2,r_3,\tau)$ to any combination of two $1s$ electrons in any of the electronic coordinates. Since this step has also removed (three times) the piece of the initial state in $1s1s1s$ we must add back in this part appropriately (twice), so that this piece is only removed once. It was found that long relaxation times (up to 20 a.u. for Li and up to 30 a.u. for Be) were required to fully complete the relaxation to the ground state.

The initial condition for the solution of the time-dependent close-coupling equations of Eq. (1) is given by

$$P^{\mathcal{L}}_{l_1l_2Ll_3}(r_1,r_2,r_3,t=0) = 0. \tag{13}$$

The three-electron close-coupling equations of Eq. (1) are a generalization of two-electron close-coupling equations used before for photon double ionization of two-electron target atoms [21,22].

The time-dependent close-coupled equations of Eq. (1) are solved using standard numerical methods to obtain a discrete representation of the radial wavefunctions and all operators on a three-dimensional lattice. Our specific implementation on massively parallel computers is to partition all the r_1, r_2, and r_3 coordinates over the many processors, so-called domain decomposition. This allows us to make use of up to thousands of processors of a supercomputer, if available. At each time step of the solution only those parts of the radial wave functions needed to calculate the second derivatives found in Eq. (2) are passed between the processors.

The probabilities for double or triple photoionization are obtained by $t\to\infty$ projection of the radial wave function onto fully antisymmetric spatial and spin functions, within double or triple summations over electron momenta (for double and triple photoionization, respectively), including the appropriate angular factors. The collision probability for triple photoionization of the ground state of Li or Be is given by

$$\begin{aligned}\mathcal{P}_{l_1l_2Ll_3,1/21/2S1/2}(t) = \sum_{k_1}\sum_{k_2}\sum_{k_3}\Bigg|&\sum_{L'}\delta_{\mathcal{L},L'}Q_aR(123,t)\\ &-\sum_{L'}(-1)^{l_2+l_3+L+L'}\sqrt{(2L+1)(2L'+1)}\begin{Bmatrix}l_2 & l_1 & L\\ l_3 & \mathcal{L} & L'\end{Bmatrix}Q_bR(132,t) - \sum_{L'}(-1)^{l_1+l_2-L'}\delta_{L,L'}Q_cR(213,t)\\ &+\sum_{L'}(-1)^{l_1+l_2+L}\sqrt{(2L+1)(2L'+1)}\begin{Bmatrix}l_2 & l_1 & L\\ l_3 & \mathcal{L} & L'\end{Bmatrix}Q_cR(312,t) + \sum_{L'}(-1)^{l_2+l_3+L'}\sqrt{(2L+1)(2L'+1)}\\ &\times\begin{Bmatrix}l_1 & l_2 & L\\ l_3 & \mathcal{L} & L'\end{Bmatrix}Q_bR(231,t)\\ &-\sum_{L'}\sqrt{(2L+1)(2L'+1)}\begin{Bmatrix}l_1 & l_2 & L\\ l_3 & \mathcal{L} & L'\end{Bmatrix}Q_aR(321,t)\Bigg|^2,\end{aligned} \tag{14}$$

where

$$R(ijk,t) = \int_0^\infty dr_1 \int_0^\infty dr_2 \int_0^\infty dr_3 \times P_{k_1 l_1}(r_i) P_{k_2 l_2}(r_j) P_{k_3 l_3}(r_k) P^{\mathcal{L}}_{l_1 l_2 L' l_3}(r_1, r_2, r_3, t) \tag{15}$$

and

$$Q_a = \sqrt{\frac{1}{2}}\delta_{S,0} - \sqrt{\frac{1}{6}}\delta_{S,1},$$

$$Q_b = \sqrt{\frac{2}{3}}\delta_{S,1},$$

$$Q_c = -\sqrt{\frac{1}{2}}\delta_{S,0} - \sqrt{\frac{1}{6}}\delta_{S,1}. \tag{16}$$

Six different terms are obtained due to the permutations of three electrons, as opposed to two permutations when only two electrons are considered. In fact, since for two electron systems the spatial and spin wave functions separate, photoionization (or excitation) probabilities can be easily obtained by projection onto simple products of one-electron radial functions, provided the two electron time-propagated radial wave function is symmetrized for singlet scattering or antisymmetrized for triplet scattering [21].

For double photoionization (with excitation) of Li, the radial part of the projections are onto products of one bound *nl* state and two continuum states, where the continuum radial wave functions are obtained by diagonalization of Eq. (11) with $V(r)$ the appropriate Hartree-Slater potential for Li. For triple photoionization of Li the radial part of the projections are made onto products of three continuum radial wave functions which are obtained by diagonalization of Eq. (11) where now $V(r) = -Z/r$. For double photoionization (with excitation) of Be, the continuum radial wavefunctions used in the radial part of the projections are obtained by diagonalization of

$$h(r) = -\frac{1}{2}\frac{\partial^2}{\partial r^2} + \frac{l(l+1)}{2r^2} + V_D(r) + V_X(r), \tag{17}$$

where $V_D(r)$ and $V_X(r)$ are the direct Hartree and local exchange potentials, respectively. For triple photoionization of Be the continuum radial wavefunction used in the radial part of the projections are obtained by diagonalization of Eq. (11). (Note that the triple photoionization of Be calculations leave the ion in the $1s$ state. No calculations leaving the ion in an excited state are possible due to our use of a frozen Be^{3+} core.) Care must be taken in the sums over the electron momenta k_2, k_3 (double photoionization) or k_1, k_2, k_3 (triple photoionization) found in the photoionization probability expression. When the associated angular momenta are equal, for example, $l_1 = l_2$, the sums must be restricted to avoid double counting of distinct continuum states. More subtle is the unwanted contribution to the probability from the continuum correlation part of two-electron bound wave functions that evolve on the lattice. This point has been discussed in detail by McCurdy *et al.* [23] in a study of the electron double ionization of an *s*-wave model He atom. Instead of projecting out two-electron bound states from the three electron time-propagated radial wave function and then projecting onto all electron momenta, we found that a simple restriction of the sums over the electron momenta, so that the conservation of energy:

$$E_{\text{atom}} + E_{\text{projectile}} - E_{nl} = \frac{k_2^2}{2} + \frac{k_3^2}{2} \tag{18}$$

for double ionization leaving the ion in an *nl* state, and

$$E_{\text{atom}} + E_{\text{projectile}} = \frac{k_1^2}{2} + \frac{k_2^2}{2} + \frac{k_3^2}{2} \tag{19}$$

for triple ionization, was approximately conserved, greatly reduced contamination from the continuum piece of the two-electron bound state wave functions. In addition, this method of restricted momenta sums should become more accurate as the lattice size increases.

Finally, the photon double and triple ionization cross section is given by

$$\sigma_\omega = \frac{\omega}{I} \sum_{l_1, l_2, l_3, L, S} \left. \frac{\partial \mathcal{P}_{l_1 l_2 L l_3, 1/2\, 1/2\, S\, 1/2}(t)}{\partial t} \right|_{t \to \infty}, \tag{20}$$

where I is the intensity of the radiation field and $\mathcal{P}$ is the total photoionization probability for either double or triple photoionization obtained previously. Care must also be taken in the sums over the quantum numbers associated with the fully antisymmetric spatial and spin wave functions to avoid double counting.

III. RESULTS

In our calculations a $(192)^3$ lattice was employed with each radial direction from $0.0 \to 19.2$ spanned by a uniform mesh with spacing $\Delta r = 0.10$ a.u. For the relaxation of the ground state, 23 channels were routinely used (up to and including $l = 3$). For Li, this gave a lattice energy of -198.76 eV, after a relaxation time of 20 a.u. Increasing the relaxation time to 30 a.u. changed this energy by a few parts in the last decimal place. One further calculation was made which included 42 channels (up to and including $l = 4$). This produced an energy of -198.77 eV after 20 a.u. of relaxation, showing that our ground state is extremely well converged with respect to the exact ground state on the lattice. The experimental Li ground state energy is -203.43 eV. Our value is within around 2% of this value. The difference between our lattice energy and the exact value is due entirely to the kinetic energy terms in Eq. (1), which are determined largely by the lattice spacing. Decreasing the mesh spacing still further would also necessarily decrease the time step employed in our propagation and result in prohibitively large calculations. However, the long relaxation times and the very good convergence of our ground-state energy with respect to the angular momenta included, shows that our initial state includes the correlation of this system very well.

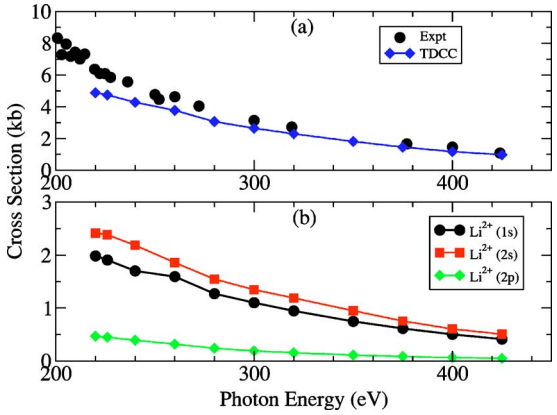

FIG. 1. (Color online) Double photoionization cross section of Li as a function of photon energy. The total double photoionization cross section is compared with the experiment of Huang *et al.* [17]. (b) The partial double photoionization cross sections leaving the Li^{2+} ion in one of three possible final states as shown (1.0 kb $=1.0\times10^{-21}$ cm^2).

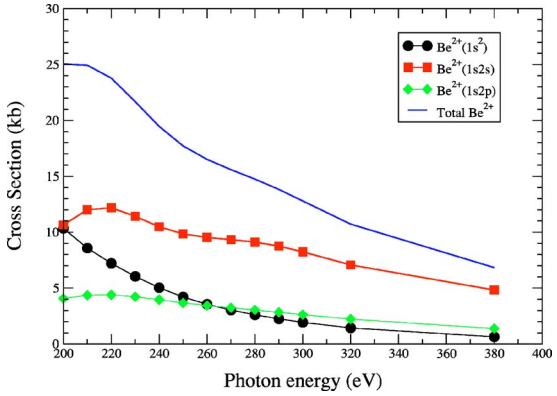

FIG. 2. (Color online) Double photoionization cross section of Be as a function of incident photon energy for time-dependent calculations including angular momentum channels up to and including $l=3$. The partial double photoionization cross section leaving the Be^{2+} ion in one of three final states is also shown (1.0 kb $=1.0\times10^{-21}$ cm^2).

For Be, it was found that larger relaxation times were necessary to fully converge the relaxation to the ground state. Using the same lattice as the Li calculations, with 23 channels, and after 30 a.u., a ground state which gave a triple photoionization threshold of −181.08 eV was found, which is well within 1% of the exact Be triple photoionization threshold. Increasing the relaxation time to 40 a.u. gave a ground-state energy of −181.10 eV. We remark that a more "exact" energy is found for Be because the Hartree-Slater potential used to calculate the Be^{2+} orbitals used in the ground state relaxation can be adjusted so that the Be^{2+} energies are almost identical to experiment.

Once a fully correlated initial state is obtained, the time-dependent close-coupling equation of Eq. (1) are propagated in real time for around 10 radiation field periods. 51 channels (up to and including $l=3$) were routinely used to represent the final $^2P^0$ state. For both atoms, one further calculation was made which included 99 channels (up to and including $l=4$) in the final state as a further convergence check. Projections were made onto fully antisymmetric spatial and spin states to obtain the necessary probabilities for double and triple photoionization. We now turn to a discussion of our results for double ionization of Li and Be, before examining the triple photoionization of Li and Be.

A. Double photoionization

It should be noted that our time-dependent calculations calculate all photoionization quantities for Li and Be. Naturally, the dominant process is single photoionization of one electron, which we do not discuss further here as these quantities are generally very well known, especially at higher photon energies. The double photoionization cross section is typically around 2 orders of magnitude lower than the single photoionization cross section. In Fig. 1 we show the double photoionization cross section for Li. In Fig. 1(a) we compare our total double photoionization cross section with the experimental measurements of Huang *et al.* [17]. Very good agreement is found with experiment, except at the lowest energies, where our calculations start to become lower than experiment. We remark that these calculations are well converged with respect to the number of channels included in the final state. A single time-dependent calculation made at an incident energy of 300 eV, which contains channels up to and including $l=4$, is almost identical to that with fewer channels. In Fig. 1(b) we show the partial double photoionization cross section leaving the Li^{2+} ion in any one of the $1s$, $2s$, or $2p$ final states. We note that the Li^{2+} ion is most likely to be left in the $1s$ or $2s$ states, with the probability of being left in the $2s$ being around 20% higher than that of being left in the $1s$. There has been recent attempts to fit the double photoionization cross section measurements for Li with a scaling model to estimate the cross sections leaving the ion in these different states [24]. It was found that our time-dependent close-coupling calculations leaving the ion in the $2s$ state were in good agreement with this fit, but that our calculations leaving the ion in the $1s$ state were around 30–40 % higher than this fit. As discussed in Ref. [24], it seems that the interference between the competing double ionization processes leaving the ion in various final states is important, and must be taken into account. A calculation or fit which treats the double ionization processes separately will not include this potentially important effect.

In Fig. 2 we show the double photoionization cross section for Be. As for Li, we also present the partial double photoionization cross sections, leaving the Be^{2+} ion in one of three final states, the $1s^2$, $1s2s$, or $1s2p$. We notice that the total double ionization cross section is quite a bit larger for Be than for Li, at the same incident photon energy. This could be related to the lower double ionization threshold for Be than for Li, caused by the screening effects of an extra inner shell electron. For Be, there are no experimental measurements with which to compare in this energy range. Previous measurements [12] and calculations [8,9] were in a much lower energy range below the threshold for ionization from the $1s$ shell.

An interesting difference in the partial double photoionization cross sections for Be is the increased likelihood of

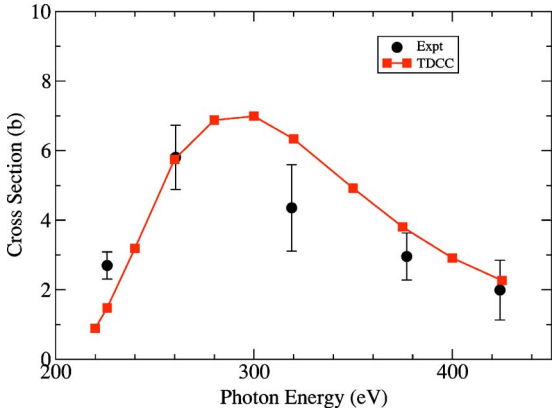

FIG. 3. (Color online) Triple photoionization cross section of Li as a function of incident photon energy. We compare the experiment of Wehlitz *et al.* [13] with our time-dependent close-coupling calculations. (1.0 b=1.0×10^{-24} cm^2).

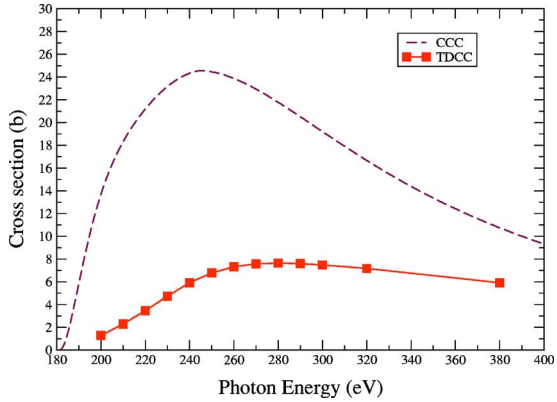

FIG. 4. (Color online) Time-dependent close-coupling calculations of the triple photoionization cross section of Be as a function of incident photon energy. We compare these calculations with the double shake-off model calculations of Kheifets and Bray [18] (dashed line) (1.0 b=1.0×10^{-24} cm^2).

double ionization leaving the ion in the Be^{2+} $1s2p$ final state. Above around 280 eV, this is more probable than leaving the ion in the $1s^2$ state. This is quite different from Li, where the probability leaving the ion in the Li^{2+} $2p$ state was much smaller than the $1s$ probability over all energies. Also, for Be, the double ionization leaving the ion in the $1s2s$ final state dominates across all energies in the range. This difference is likely due to the strong mixing between $1s^22s^2$ and $1s^22p^2$ in the initial Be ground state, which increases the probability that the Be^{2+} ion can be left in the $1s2p$ final state. This is not present in the ground state of Li, where the ground $1s^22s$ state does not mix with the $1s^22p$ state, explaining the lower probability of double ionization of Li leaving the ion in the $2p$ final state. This underscores the importance of including correlation effects in the initial state of the system when considering multiple ionization processes.

B. Triple photoionization

We now examine the triple photoionization cross section. It should be emphasized that these results come from the same calculations which produce the double photoionization cross section. The same time-dependent propagation is used, but the projections used to get the probabilites are different for double and triple ionization, as discussed following Eq. (16). Again, the triple photoionization cross section is typically three orders of magnitude lower than the double photoionization cross section.

In Fig. 3 we show the triple photoionization cross section for Li, and compare it with the experimental measurements of Wehlitz *et al.* [13]. Our calculations which include 51 channels up to and including $l=3$ are shown by the red line. These are in good agreement (within the error bars) for three of the five experimental points. At 225 and 320 eV incident photon energy, our calculations are just outside the error bars. We also note that our calculations are in good agreement with very recent calculations [25] using classical trajectory methods. It was discussed in our previous paper on Li [16], that our calculations for the triple photoionization were not converged with respect to the highest angular momenta of the number of channels included. This was based on the comparison of calculations including up to $l=2$ with those including $l=3$. The calculations including up to $l=3$ were higher by around 50% than those with $l=2$. It was then decided to attempt a calculation which included up to $l=4$, which required 99 channels in the final state. This quickly becomes an enormous calculation, made even larger by the extra time required for the many projections which now must be made (resulting from the large increase in the number of determinantal states) in order to compute the ionization probabilities. However, one such calculation at an incident energy of 300 eV was completed by utilizing several thousand supercomputing processors available to us. The triple photoionization cross section resulting from this calculation was around 30% higher than the cross section computed including channels up to $l=3$. This is disappointing, as the double photoionization cross section resulting from the same calculation is well converged by including angular momenta up to and including $l=3$. It seems that this triple photoionization cross section is a very difficult quantity to converge, perhaps due to the extremely small nature of this cross section (barns). An even larger calculation which would include all channels up to $l=5$ is not yet possible given current computational resources. It is also possible that a larger radial mesh is needed to include these $l=4$ orbitals which are more spatially extended. Also, calculations with a finer mesh, which may become important for orbitals which approach the nucleus, may lead to improved convergence with respect to the angular momenta. Both these calculations will be attempted once the necessary computing resources become available.

Finally in Fig. 4, we examine the triple photoionization of Be, where now we can compare with the double shake-off model calculations of Kheifets and Bray [18]. Clearly our time-dependent calculations (which were made including all channels up to and including $l=3$) are quite a bit lower than the model calculations. Also, the peak of the cross section is higher for the time-dependent calculations (around 280 eV) than for the model calculations (around 250 eV). Interest-

ingly, it appears that our triple photoionization cross sections for Be are better converged than the calculations for Li. The calculations including all channels up to $l=3$ are around 20–30 % higher than those including all channels up to $l=2$. A single calculation including all channels up to $l=4$ at 280 eV incident photon energy is around 20% higher than the $l=3$ calculation.

It seems therefore that our time-dependent calculations are lower than those found by using the double shake-off model. Even though our triple photoionization cross sections are not completely converged, they are clearly much lower than the double shake-off model results. The magnitude of the triple photoionization cross section for Be is quite similar to that for Li. This is unlike the double ionization where the Be cross section was quite a bit larger than the Li double ionization cross section. This could be due to the fact that the triple ionization thresholds are fairly similar for Li and Be (203 and 181 eV, respectively), whereas the double ionization thresholds are quite different (81 and 27 eV, respectively).

IV. SUMMARY

In conclusion, we have extended our time-dependent calculations of three-electron systems to examine further the Li atom and to calculate double and triple photoionization cross sections for Be. We find our double ionization cross sections to be well converged and in good agreement with available experimental results. For triple ionization, the cross section appears to be more slowly convergent for Li, although for Be the triple ionization seems to converge somewhat faster. Our triple photoionization cross sections for Be are over a factor of 2 lower than a previous double shake-off model calculation. We look forward to utilizing the steady increase in computing power so that larger three-electron calculations can be made. We also are implementing our three-electron algorithms to further studies of electron-impact double ionization [19] and double autoionization problems [20].

ACKNOWLEDGMENTS

We thank A. Kheifets for supplying his results in numerical form. This work was supported in part by DOE Grant No. DE-FG05-99ER5438 and DOE SciDAC Grant No. DE-FG02-01ER54G44 to Auburn University. A portion of this work was performed under the auspices of the U.S. Department of Energy through the Los Alamos National Laboratory. Computational work was performed at the National Energy Research Scientific Computing Center (NERSC) at Oakland, CA, and at the National Center for Computational Sciences in Oak Ridge, TN. In particular, we thank the consultants at NERSC for their invaluable advice and support in running large memory and time-intensive jobs on the NERSC supercomputing platforms.

[1] J. S. Briggs and V. Schmidt, J. Phys. B **33**, R1 (2000).
[2] A. S. Kheifets and I. Bray, J. Phys. B **31**, L447 (1998).
[3] L. Malegat, P. Selles, and A. K. Kazansky, Phys. Rev. Lett. **85**, 4450 (2000).
[4] J. Colgan, M. S. Pindzola, and F. Robicheaux, J. Phys. B **34**, L457 (2001).
[5] C. W. McCurdy, D. A. Horner, T. N. Rescigno, and F. Martin, Phys. Rev. A **69**, 032707 (2004).
[6] H. Bräuning, R. Dörner, C. L. Cocke, M. H. Prior, B. Krässig, A. S. Kheifets, I. Bray, A Brauning-Demian, K. Carnes, S. Dreuil, V. Mergel, P. Richard, J. Ullrich, and H. Schmidt-Böcking, J. Phys. B **31**, 5149 (1998).
[7] A. Knapp, A. Kheifets, I. Bray, T. Weber, A. L. Landers, S. Schössler, T. Jahnke, J. Nickles, S. Kammer, O. Jagutzki, L. P. H. Schmidt, T. Osipov, J. Rösch, M. H. Prior, H. Schmidt-Böcking, C. L. Cocke, and R. Dörner, Phys. Rev. Lett. **89**, 033004 (2002).
[8] A. S. Kheifets and I. Bray, Phys. Rev. A **65**, 012710 (2001).
[9] J. Colgan and M. S. Pindzola, Phys. Rev. A **65**, 022709 (2002).
[10] F. Citrini, L. Malegat, P. Selles, and A. K. Kazansky, Phys. Rev. A **67**, 042709 (2003).
[11] D. Lukić, J. B. Bluett, and R. Wehlitz, Phys. Rev. Lett. **93**, 023003 (2004).
[12] R. Wehlitz, D. Lukić, and J. B. Bluett, Phys. Rev. A **71**, 012707 (2005).
[13] R. Wehlitz, M. T. Huang, B. D. DePaola, J. C. Levin, I. A. Sellin, T. Nagata, J. W. Cooper, and Y. Azuma, Phys. Rev. Lett. **81**, 1813 (1998).
[14] H. W. van der Hart and C. H. Greene, Phys. Rev. Lett. **81**, 4333 (1998).
[15] T. Pattard and J. Burgdörfer, Phys. Rev. A **63**, 020701 (2001).
[16] J. Colgan, M. S. Pindzola, and F. Robicheaux, Phys. Rev. Lett. **93**, 053201 (2004).
[17] M. T. Huang, R. Wehlitz, Y. Azuma, L Pibida, I. A. Sellin, J. W. Cooper, M. Koide, H. Ishijima, and T. Nagata, Phys. Rev. A **59**, 3397 (1999).
[18] A. S. Kheifets and I. Bray, J. Phys. B **36**, L211 (2003).
[19] M. S. Pindzola, F. J. Robicheaux, J. P. Colgan, M. C. Witthoeft, and J. A. Ludlow, Phys. Rev. A **70**, 032705 (2004).
[20] M. S. Pindzola, F. Robicheaux, and J. Colgan, Phys. Rev. A (to be published).
[21] M. S. Pindzola and F. Robicheaux, Phys. Rev. A **57**, 318 (1998).
[22] J. Colgan and M. S. Pindzola, Phys. Rev. Lett. **88**, 173002 (2002).
[23] C. W. McCurdy, D. A. Horner, and T. N. Rescigno, Phys. Rev. A **65**, 042714 (2002).
[24] R. Wehlitz, J. Colgan, M. M. Martinez, J. B. Bluett, D. Lukić, and S. B. Whitfield, J. Electron Spectrosc. Relat. Phenom. **144–147**, 59 (2005).
[25] A. Emmanouilidou and J. M. Rost, physics/0409034 (unpublished).